TANDEM-L PERFORMANCE ANALYSIS FOR THREE DIMENSIONAL EARTH DEFORMATION MONITORING

Homa Ansari[(1,2)] , Kanika Goel[(1)], Alessandro Parizzi[(1)], Francesco De Zan[(1)], Nico Adam[(1)], Michael Eineder[(1,2)]

(1) Chair of Remote Sensing Technology, Technical University of Munich (TUM), Munich, Germany
(2) Remote Sensing Technology Institute (IMF), German Aerospace Center (DLR), Wessling, Germany

ABSTRACT

Interferometric synthetic aperture radar (InSAR) measurements are merely sensitive to the deformation along the Line of Sight (LOS) direction of the sensor. To improve the geometrical sensitivity and retrieve the three-dimensional deformation, the integration of InSAR from non-coplanar acquisitions as well as fusion with resolution-scale SAR image shift measurements has become a standard approach. Using different statistical measures, we assess and compare the influence of different image acquisition strategies as well as data fusion on the performance of InSAR in 3D deformation retrieval. Integrating nominal InSAR acquisitions, i.e. a set of measurements from ascending and descending tracks acquired from right-looking geometry, a strong correlation between the retrieved 3D parameters in the local vertical-north plane is observable. This correlation is sought to be decreased by non-nominal acquisitions; i.e. left-looking or squinted observations. These acquisition strategies are discussed for consideration in the future L-band mission Tandem-L.

Index Terms- Three-dimensional deformation, InSAR, Azimuth shifts, SAR acquisition geometry, Error analysis.

1. INTRODUCTION

Tandem-L is a proposal from the German Aerospace Center (DLR) for future L-band synthetic aperture radar (SAR) satellite mission which enables continuous high resolution monitoring of the earth surface dynamics [1]. As part of the phase-A study of the mission, the current work attempts to identify the data acquisition's geometrical parameters relevant to the achievable accuracy of the 3D earth surface deformation and to assess their effect on the improvement of this accuracy.

The side looking image acquisition of SAR system merely allows the interferometric approaches to capture the projection of the 3D deformation to the line of sight (LOS) direction of the sensor. In order to retrieve the 3D deformation, InSAR from different acquisitions is combined. In previous studies, the fusion of InSAR from ascending/descending acquisitions, hereafter referred to as *cross-heading tracks*, and their impact on the achievable 3D performance has been introduced in [2] and [3]; leading to the conclusion that the fusion of cross-heading acquired from right and left-looking enhances the precision.

Although effective in 3D decomposition, the left-looking acquisition scenario imposes expensive trade-offs for the mission acquisition planning. Thus, on one hand, it is of interest to know in what aspects and to what extent the 3D deformation retrieval benefits from the left-looking acquisition scenario. On the other hand, it is important to investigate alternative acquisition possibilities which may enhance the 3D retrieval and substitute the expensive left-looking acquisition scenario. As an extension of the works in [2] and [3], the focus of the current study is therefore on addressing the different possible acquisition and fusion scenarios and introducing statistical measures for comparing the corresponding InSAR 3D performance of current and future SAR missions.

The problem is assessed in two different aspects: first by investigation of the achievable accuracy for independent pointwise decomposition of the deformation and second by assessing the impact of the InSAR 3D performance on modeling the common deformation sources in case of volcanic and seismic activities. The former is treated extensively in the second and third section of the current work, while the latter is briefly introduced in the fourth section and extensively treated in a separate work [4].

2. INSAR IN 3D DEFORMATION RETREIVAL

The LOS deformation observed by InSAR can be expressed as the inner product of the three dimensional deformation and LOS unit vector [5]:

$$d_{LOS} = \boldsymbol{e}_{LOS} \cdot \boldsymbol{d}, \quad (1)$$

where $\boldsymbol{d}$ is the three dimensional deformation vector in the local Cartesian coordinate system defined by the local east, north and vertical directions: $\boldsymbol{d} = [d_e, \ d_n, \ d_v]^T$ and $\boldsymbol{e}_{LOS}$ is a function of the satellite heading α and antenna look angle θ.

The differential image shifts in azimuth direction, hereafter referred to as the *azimuth shifts*, can also be utilized to retrieve the deformation signal; although with lower precision compared to the InSAR. These measurements are obtained by various techniques such as cross-correlation [6], exploitation of spectral diversity [7],[8] etc.. In this case, the deformation is mapped to the along-track direction of the satellite as:

$$d_{Az} = \boldsymbol{e}_{Az} \cdot \boldsymbol{d}, \quad (2)$$

with $\boldsymbol{e}_{Az}$ as a function of the satellite heading angle α.

To retrieve the three deformation components, at least three independent observations are required. These observations may be from three non-coplanar acquisition geometries [1]; using a pure interferometric approach, or from two different geometries; using the fusion of interferometric and azimuth shift measurements. The latter is however limited to high magnitude deformation signals where the high noise of the azimuth shifts still allows the detection

Case	Fusion Scenario	Heading ang. (at Equator)	Look ang.	3D precision (at Equator)
I	Asc. R.	-12°	43°	σ_e: 0.018
	Desc. R.	-168°	43°	σ_n: 0.249
	Asc. R.	-12°	23°	σ_v: 0.041
II	Asc. R.	-12°	43°	σ_e: 0.018
	Desc. R.	-168°	43°	σ_n: 0.105
	Asc. R. Squinted	-12° (-20°)	23°	σ_v: 0.017
III	Asc. R.	-12°	43°	σ_e: 0.018
	Desc. R.	-168°	43°	σ_n: 0.074
	Asc. L.	-12	-23°	σ_v: 0.011
IV	Asc. R. + Az. Sh.	-12°	43°	σ_e: 0.018
	Desc. R. + Az. Sh.	-168°	43°	σ_n: 0.217
	Asc. R. + Az. Sh.	-12°	23°	σ_v: 0.037
V	Asc. R. + Az. Sh.	-12°	43°	σ_e: 0.016
	Desc. R. + Az. Sh.	-168°	43°	σ_n: 0.038
	Asc. R. + Az. Sh.	-12°	23°	σ_v: 0.013

Table 1. Selected geometrical fusion scenarios and the resulted 3D deformation error at Equator; Azimuth resolution is case IV and V are 10 and 2 m, respectively

of the geophysical signal.

3D deformation is retrieved by weighted least squares as follows:

$$y_i = \left[d_{Az,i} \quad \text{or} \quad d_{LOS,i}\right], \qquad \boldsymbol{a}_i = \left[\boldsymbol{e}_{Az,i} \quad \text{or} \quad \boldsymbol{e}_{LOS,i}\right],$$

$$A = [\boldsymbol{a}_1, \boldsymbol{a}_2, \dots, \boldsymbol{a}_n]^T,$$

$$\boldsymbol{d} = \left(A^T Q_y^{-1} A\right)^{-1} . A^T Q_y^{-1} \boldsymbol{y} \ , \qquad (3)$$

where vector $\boldsymbol{y}$ contains the observed deformation, matrix A is defined by the respective measurements' direction: i.e. $\boldsymbol{e}_{Az,i}$ or $\boldsymbol{e}_{LOS,i}$ and Q_y is the covariance matrix introducing the measurements' stochastic model. Having independent measurements, a diagonal matrix, with measurements' variance as its elements, can best describe the stochastic model. For error analysis purposes, the measurements' stochastics is approximated by the Cramer Rao Bounds of the interferometric [9] and azimuth shift [10] measurements, i.e.:

$$\sigma^2_{0,LOS} = \frac{1-\gamma^2}{2N\,\gamma^2}\left(\frac{\lambda}{4\pi}\right)^2, \qquad (4)$$

$$\sigma^2_{0,\mathrm{Az}} = \frac{3}{2N} \cdot \frac{1-\gamma^2}{(\pi\,\gamma)^2} \cdot \rho^2_{az}\,, \qquad (5)$$

respectively; introducing γ as signal coherence, N as the number of samples exploited in estimation of the measurements, ρ_{Az} as the SAR resolution in azimuth direction and λ as the SAR wavelength.

Having this fusion setup, the estimation covariance matrix can be utilized as the statistical measure for assessing the 3D performance:

$$Q_d = \left(A^T Q_y^{-1} A\right)^{-1} = \begin{bmatrix} \sigma_e^2 & \sigma_{en} & \sigma_{ev} \\ \sigma_{en} & \sigma_n^2 & \sigma_{nv} \\ \sigma_{ev} & \sigma_{nv} & \sigma_v^2 \end{bmatrix} \qquad (6)$$

Q_d is a square symmetric matrix serving as the initial point of the error assessment; with its diagonal elements approximating the

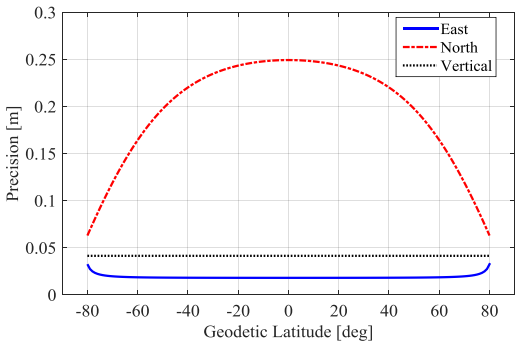

Fig. 1. Nominal geometric scenario (Tab. 1, case I): 3D precision as a function of geodetic latitude

estimation error variance and its 2×2 submatrices representing the second-order statistics of the joint bivariate probability density function (PDF) between the parameter pairs. Assuming Gaussian stochastics, the joint PDFs are further visualized and served as a comparison tool in our analysis, as follows: applying the eigenvalue decomposition of the aforementioned submatrices, the eigenvalues (λ_1, λ_2) and eigenvectors $(\boldsymbol{v}_1\,, \boldsymbol{v}_2)$ yield:

$$q_{i,j} = \begin{bmatrix} \sigma_i^2 & \sigma_{i,j} \\ \sigma_{i,j} & \sigma_j^2 \end{bmatrix} \rightarrow \quad q_{i,j} \;=\; \sum_{k=1}^{2} \quad \lambda_k \;\boldsymbol{v}_k \boldsymbol{v}_k{}^T \quad (7)$$

Based on the decomposition results, the error ellipses are then formed; with the λ_1, λ_2 as their semi major and minor axes elongated in the direction specified by the corresponding eigenvectors. The orientation of the ellipse represents the correlation between the two parameters.

3. THE EFFECT OF ORBIT AND ACQUISITION GEOMETRY ON 3D PERFORMANCE

As apparent from equations (1) and (5), the 3D performance is a function of sensor's orientation, namely the satellite heading and the antenna look angle. The effect of each mentioned governing factors on the deformation accuracy is assessed separately in the following subsections.

To keep the investigated cases comparable, a basic combination scenario is assumed: comprised of three measurements with two fixed cross-heading right-looking acquisitions; and the third acquisition kept variable according to the geometric case under study (Table 1). Without loss of generality, we consider an L-band SAR with average coherence of 0.4 for calculation of the measurements' noise according to Eq. 4. This merely has a scaling effect on the error analysis.

3.1 Impact of the satellite heading angle

The heading angle varies by the satellite orbit and attitude, and depends on the orbital inclination, type of the satellite track (ascending/descending), the latitude of the imaged scene and the squint angle of the antenna [11].

Being an earth observation mission with global coverage objective, the SAR missions are mostly limited to a low-earth, near-circular, near-polar, sun-synchronous orbit. The choice of inclination is thus limited and coupled with the satellite altitude as well as the orbital eccentricity [12]. For instance for a near circular orbit (eccentricity

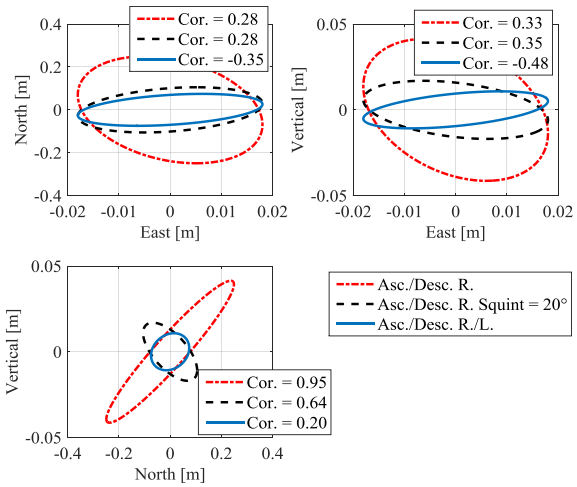

Fig. 2. Comparison of the nominal and non-nominal acquisition scenarios through the error ellipses; the error ellipses indicate an extreme correlation in the vertical-north plane when considering the nominal acquisitions, the correlation reduces by considering the squinted or left-looking acquisition

= 0.001) the inclination is allowed between [97.3° to 98.6°] for low earth orbits' altitude of [500 to 800] km. This diversity in inclination; and consequently on the heading angle, has a negligible impact on improving the 3D precision. In contrast to the change in inclination, the change in the track type, i.e. the combination of ascending and descending tracks has a key role in 3D deformation retrieval [3], thus is kept as a baseline for the comparisons.

Having the nominal combination scenario of (Table 1-Case I), the heading angle is calculated for different geodetic latitudes. The 3D precision obtained from the calculated heading angle is depicted in Fig. 1. As seen from the figure, retrieving the north component is the most critical due to the choice of near-polar orbit and poor sensitivity of InSAR to the along-track direction of the satellite. It is also evident that the accuracy decreases toward mid-latitudes and is worst at the equator. To further assess the performance, the corresponding error ellipses at the equator are shown in Fig. 2. The error ellipse of the vertical-north components reveals an extreme correlation between the two components which indicates the ambiguity in retrieving the mentioned parameters under the assumed combined acquisition scenario.

To assess the effect of squint angle, it is changed in the [0° to 20°] range and the obtainable accuracy is reported (Fig. 3; presented at fix latitude (0°)). The figure reveals a gain of nearly 8 dB in the accuracy of the north component; while the comparison between the error ellipses in case of squinted acquisitions with non-squinted case (Fig. 2) reveals 30 percent decrement of the extreme correlation in the vertical-north plane.

3.2. Impact of the antenna look angle

Dependent on the mission capabilities, the look angle may be varied by the platform in the range of [20° to 50°]. The platform may also allow for two modes of right and left-looking acquisition by rotation around its roll axis. There are therefore two different possibilities in improving the angular diversity of the look-angle: either by combination of acquisitions from different look-angles all

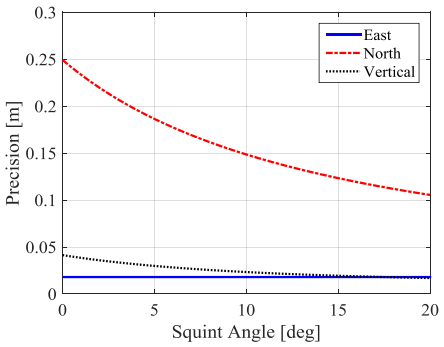

Fig. 3. Squinted geometric scenario (Tab. 1, case II): 3D precision at Equator; the retrieval of north component benefits from the single squint acquisition

acquired from right or by combining the right and left-looking acquisitions.

As it has been discussed in [2], the left-looking acquisition provides a larger angular diversity and is thus more advantageous in 3D retrieval. In order to study this effect, we adapt the nominal combination scenario of case I and change the third acquisition to a left-looking (Table 1, case III).

Comparing the performance of nominal and left-right geometric fusion, the performance gain especially in the north component is apparent. Fig. 2 reveals another advantage of the left-looking acquisition, namely the decoupling of the parameters in the vertical-north plane which is evident from decreasing the extreme correlation by more than 70 percent.

4. THE EFFECT OF MEASUREMENT FUSION

Providing sensitivity to the along-track direction, the azimuth shifts are geometrically complementary to the interferometric measurements. The low resolution of these measurements, however, limits their contribution to the data fusion in 3D retrieval.

The quality of the azimuth shifts depends both on: the azimuth resolution of SAR; and the spatial homogeneity of the deformation signal. The latter affects the size of the estimation window (hence the number of samples) for obtaining the azimuth shifts [10]. On the other hand, the relative contribution of the shifts compared to the interferometric measurements is merely governed by the ratio of azimuth resolution to half the wavelength [10]. Therefore, the fusion of azimuth shifts is more advantageous in cases of long-wavelength SAR with high azimuth resolution.

To study the information enhancement obtained from the azimuth shifts, a deformation signal smooth enough to allow for a 50 × 50 m² estimation window is assumed. Similar to the previous section we consider an L-band SAR with coherence of 0.4 for weighting the measurements according to equation (4) and (5). We again adapt our basic cross-heading right-looking scenario. With the difference that here for each acquisition, both azimuth shifts and interferometric measurements are integrated in the 3D retrieval. We further consider and compare two extreme cases: in the first, the azimuth resolution is five times worse than the range resolution (ρ_{az}= 10 m; Table 1, case IV), while in the second an identical azimuth and range resolution is considered (ρ_{az}= 2 m; Table 1, case V). Fig. 4 depicts the error ellipses of the two mentioned cases compared to the nominal scenario of case I; for an equatorial region. As expected, the impact of the azimuth shift measurements is in close relation to the azimuth resolution. If this resolution is high enough to allow high quality deformation

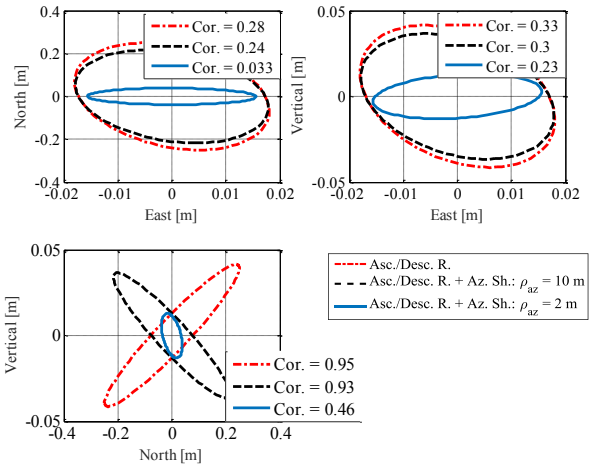

Fig. 4. 3D performance gain in fusion of the InSAR and azimuth shifts, comparing two cases with azimuth resolution of 10 and 2 m; in extreme cases of low azimuth resolution the 3D precision and decoupling of parameters is comparable to non-nominal geometric acquisitions

measures (as is the case in $\rho_{az} = 2$m), the 3D retrieval benefits from the integration of azimuth shifts; the precision of deformation components improve in each direction while the mutual correlations decrease.

5. MULTI-ASPECT SAR IN DEFORMATION SOURCE MODELING

The deformation signal obtained by InSAR can be related to an appropriate geophysical model which describes the deforming phenomenon. To assess the necessity and effect of multi-aspect InSAR in geophysical modeling, two commonly used deformation models in case of seismic and volcanic activities; namely, the Okada and Mogi point source, are assumed respectively.

It is well-known that the combination of cross-heading tracks improves the accuracy of respective models' parameters. The main question to be answered is whether the poor sensitivity of InSAR to the north deformation component and the high correlation between the vertical-north deformation components can affect the precision of geophysical modeling; and in case of such impact, can the improvement in 3D performance lead to more precise geophysical modeling.

Our analysis on the aforementioned models reveals that depending on the share of the north component in the total deformation, the modeling precision is compromised. In such cases the consideration of left-looking geometry can improve the modeling precision while decreasing the correlations of the model parameters. The detailed explanation of the comparison strategy and review of the obtained results is reported in a separate work [4].

6. DISCUSSION AND CONCLUSIONS

In retrieving the 3D deformation signal, two distinctive geometrical scenarios have been compared. Table 1 summarizes the considered geometric scenarios as well as the achievable 3D deformation precision in the worst-case i.e. at equatorial regions.

The left-looking acquisition has been shown to best resolve the extreme correlation of the north-vertical deformation components while decreasing the 3D estimation error. This acquisition mode however imposes additional attitude maneuvers leading to comprise of the temporal-resolution of the acquisition.

The squinted-acquisition proves to improve the precision of 3D retrieval and decrease the parameter correlation; to a lesser extent in comparison with the left-looking, but with no additional costs for the mission per se; the trade-off here is however on the data processing level and complication of the SAR signal processing algorithms [11].

Investigating the performance of SAR data fusion, i.e. the integration of interferometric and azimuth shifts in the 3D retrieval, indicates the dependency of the performance on the azimuth resolution of the images. In extreme cases of high azimuth resolution the azimuth shifts can enhance the 3D precision and decrease the parameter correlation, this result is however dependent on the spatial correlation of the deformation signal as well as the SAR wavelength.

As a follow-up analysis, the effect of achievable pointwise 3D deformation precision on the performance of InSAR-based geophysical modeling is under study and the intermediate results are reported in [4].

REFERENCES

[1] I. Hajnsek, M. Shimada,M. Eineder, K. Papathanassiou, T. Motohka, M. Watanabe, M. Ohki et al. "Tandem-L: Science Requirements and Mission Concept", In *Proceedings of EUSAR 2014; 10th European Conference on Synthetic Aperture Radar*, pp. 1-4, 2014.

[2] F. Rocca, "3D motion recovery with multi-angle and/or left right interferometry," *Proceedings of the third International Workshop on ERS SAR*, 2003.

[3] T.J. Wright, B.E. Parsons, and Z. Lu, "Toward mapping surface deformation in three dimensions using InSAR," *Geophysical Research Letters* vol 31, no. 1, 2004.

[4] H. Ansari, K. Goel, A. Parizzi, H. Sudhaus, N. Adam, M. Eineder, "InSAR Sensitivity Analysis of Tandem-L Mission for Modeling Volcanic and Seismic Deformation Sources", *FRINGE Workshop 2015*, Frascati, Italy, 23-27 March 2015.

[5] R.F. Hanssen, *Radar interferometry: data interpretation and error analysis*, Springer, Dordrecht, the Netherlands, 2001.

[6] A.L. Gray, K.E. Mattar, P.W. Vachon, R. Bindschadler, K.C. Jezek, R. Forster, and J.P. Crawford, "InSAR results from the RADARSAT Antarctic Mapping mission data: Estimation of Glacier Motion Using a Simple Registration Procedure," *Proceedings of Geoscience and Remote Sensing Symposium, Seattle*, USA, Vol. 3, pp. 1638-1640, 1998.

[7] R. Scheiber, and A. Moreira, "Coregistration of interferometric SAR images using spectral diversity," *IEEE Transactions on Geoscience and Remote Sensing*, vol. 38, no. 5, pp. 2179–2191, 2000.

[8] N.B.D. Bechor and H.A. Zebker, "Measuring two-dimensional movements using a single InSAR pair," *Geophysical Research Letters*, vol. 33, no. 16, 2006.

[9] R. Bamler, and P. Hartl, "Synthetic aperture radar interferometry," *Inverse problems*, vol. 14, no. 4, 1998.

[10] R. Bamler, and M. Eineder, "Accuracy of differential shift estimation by correlation and split-bandwidth interferometry for wideband and delta-k SAR systems," *IEEE Geoscience and Remote Sensing Letters*, vol. 2, no. 2, pp. 151-155, 2005.

[11] I. G. Cumming, and F. H. Wong, *Digital Processing Of Synthetic Aperture Radar Data: Algorithms And Implementation.* Artech House Remote Sensing Library, 2005.

[12] R. J. Boain, *AB-Cs of Sun-Synchronous Orbit Mission Design*, Jet Propulsion Laboratory, National Aeronautics and Space Administration, 2004.